EUR 3627e

EUROPEAN ATOMIC ENERGY COMMUNITY - EURATOM

WEAR MEASUREMENTS
BY MEANS OF γ -X-FLUORESCENCE

by

A. KEMPER
(TNO)

1967

EUR 3627 e

WEAR MEASUREMENTS BY MEANS OF γ-X-FLUORESCENCE
by A. KEMPER (TNO)

European Atomic Energy Community — EURATOM
Report prepared by the TNO
Organisatie voor Toegepast Natuurwetenschappelijk Onderzoek
Delft (Netherlands) — Central Laboratory
Euratom Contract No. 036-64-7 IRAN
Brussels, October 1967 — 44 Pages — 15 Figures — FB 60

The excitation of X-rays by gamma radiation, so called " γ-X-fluorescence ", can be applied to wear measurements by placing, for example, a γ-source plus an X-ray detector on one side of the wearing material and an (non-radioactive) X-ray target inside or on the other side of the wearing material. The attenuation of the characteristic X-rays excited in the target, can be a measure of the (varying) thickness of the wearing layer.

The use of radioisotopes is restricted to the time required for the measurements, so the hazards of radiation and contamination are not present.

A rubber flooring compound of 1.6 mm thickness has been chosen for the evaluation of the method, since a practical performance trial with this material could be conducted under relatively plain and simple conditions in addition to the laboratory experiments.

The procedure in an actual wearing experiment is simple. Targets of silver sheet are applied at interesting points under the flooring tiles and left in position. A measuring probe is placed on the flooring on top of the targets after certain intervals of time depending on the traffic density and the wear rate expected. Then the Ag-KX-signal is registered by single-channel counting. Wear can be assessed by comparing this signal with a calibration graph established in the laboratory.

A portable probe containing an Am-241 source and a shielded detector part has been developed. This probe can be operated in connection with commercially available analyzing equipment.

EUR 3627e

EUROPEAN ATOMIC ENERGY COMMUNITY - EURATOM

WEAR MEASUREMENTS
BY MEANS OF γ -X-FLUORESCENCE

by

A. KEMPER
(TNO)

1967

SUMMARY

The excitation of X-rays by gamma radiation, so called "γ-X-fluorescence", can be applied to wear measurements by placing, for example, a γ-source plus an X-ray detector on one side of the wearing material and an (non-radioactive) X-ray target inside or on the other side of the wearing material. The attenuation of the characteristic X-rays excited in the target, can be a measure of the (varying) thickness of the wearing layer.

The use of radioisotopes is restricted to the time required for the measurements, so the hazards of radiation and contamination are not present.

A rubber flooring compound of 1.6 mm thickness has been chosen for the evaluation of the method, since a practical performance trial with this material could be conducted under relatively plain and simple conditions in addition to the laboratory experiments.

The procedure in an actual wearing experiment is simple. Targets of silver sheet are applied at interesting points under the flooring tiles and left in position. A measuring probe is placed on the flooring on top of the targets after certain intervals of time depending on the traffic density and the wear rate expected. Then the Ag-KX-signal is registered by single-channel counting. Wear can be assessed by comparing this signal with a calibration graph established in the laboratory.

A portable probe containing an Am-241 source and a shielded detector part has been developed. This probe can be operated in connection with commercially available analyzing equipment.

KEYWORDS

MATERIALS TESTING
WEAR
GAMMA SOURCES
X RADIATION
FLUORESCENCE
AMERICIUM 241
RUBBER
RADIOISOTOPES
EXCITATION
TARGETS
SILVER

Nondestructive Testing

Contents :

WEAR MEASUREMENTS BY MEANS OF γ-X-FLUORESCENCE

1. INTRODUCTION **)

Radioisotope induced X-ray fluorescence has been steadily acquiring a place
of its own alongside conventional X-fluorescence equipment. In the latter case a
sample is exposed to the output of an X-ray tube requiring high tension, stabili-
zation and cooling; characteristic sample signals can then be isolated by a dif-
fraction procedure, due to the high initial intensity of the exciting X-rays.
Radioisotope excitation, however, based mainly as it is on stable *) sources of
photons or β-particles, permits the use of simpler, cheaper and more portable
apparatus at the cost of lower initial intensity. Since, for the latter reason,
diffraction separation is not possible, one has to rely on the resolution of
detector and electronic equipment. Yet X-rays of a certain element can be counted
in the presence of neighbouring elements by additional application of selective
absorption filters[1].

A transportable fluorescence probe makes non-destructive testing possible,
whereas in the case of heavy conventional X-fluorescence equipment samples have
to be specially prepared and brought to the X-ray tube.

Radioisotope induced X-fluorescence is being applied for a number of practical
quantitative problems, such as element control of alloys, minerals, cement raw mix
and exhaust gases of industrial furnaces, the assessment of silver in photographic
emulsions, measurement of coating thickness etc. A curiosity is the qualitative
gold detector in customs control[2][3][4].

Commercial equipment is available for the determination of metal coatings on
metal base[5][6] and for general analytical applications in connection with sorting
problems and production control[7].

A new application of this relatively simple X-fluorescence technique is illus-
trated in the present report. The possibility of non-destructive wear-control has
been studied as a general problem. Flat rubber flooring-tiles have been used as
special test material in laboratory calibrations and in an experiment carried out
in an office building under conditions of actual practice.

_____

*) Decay can be accounted for if necessary.

**) Manuscript received on August 9, 1967.

It is advisable to define the aims of non-destructive wear control as far as this can be done in general terms. Usually it makes no sense to state an object's obvious strong wear in a more or less final state. In most cases producers or users of materials prefer to compare the wear-resistance of competing compounds after short intervals.

To predict wear properties of materials, wear must either be accelerated, which is a doubtful business, or wear must be continued for periods long enough to observe any wear under actual circumstances. If smaller quantities of wear can be detected, more information can be acquired over the same period of measurement or this period can be shorter.

A destructive wear test requires more samples than a non-destructive method of evaluation, since it is usually not known when to expect the first measurable effect. Furthermore, a non-destructive test like the one described here enables the investigator to continue his measurements on the same samples and thus to observe the wear rate under favourable conditions of reproducibility and under actual conditions of practice.

2. PRINCIPLE OF THE METHOD AS APPLIED TO WEAR EVALUATION

Thickness gauging in transmission geometry is more accurate than the back-scatter method. Application of a radioisotope source into or onto a wearing object would, however, mean a serious complication. It is for this reason that a combination of both principles has been chosen.

A suitable target is placed in or under the object studied and a measuring probe containing radioisotope source and detector is placed on top of the object. The target is excited by the radiation of the source to yield its characteristic X-rays and to serve as a secondary source. These X-rays are attenuated in trans-mission through the object and the detector signal therefore measures the (varying) thickness of the wearing object. It is, of course, a necessary condition for quantitative interpretation of measurements that the probe can be placed in a reproducible fixed position with respect to the target.

Fig. 1 contains a schematic presentation of the set-up chosen.

3. CHOICE OF RADIOISOTOPE SOURCE AND TARGET

3.1. Radioisotope source

The isotope to be chosen should be a low energy emitter (< 100 keV) preferably with no higher energies present, since these would increase detector noise and might cause overload pulses.

Beta-emitters as such, or mounted as Bremsstrahlung sources are considered less suitable for the purpose of wear control by thickness gauging as described. The excitation of characteristic X-rays would in both cases be accompanied by a relatively large amount of continuous Bremsstrahlung background, reducing the accuracy of channel counting owing to an absolute increase in statistical standard deviation. To compensate for this, source strength would have to be increased, which cannot be recommended in case of a portable measuring head.

Gamma- and/or X-emitting nuclides offer the advantage of relatively less scattering and of better penetration of the exciting rays down to the target. Application of the following low energy γ-emitters may be considered:

3.1.1. Cd-109 (88 keV-γ and 22 keV-X-rays)

There is a number of disadvantages. The half-life is short (1.3 y) and gamma emission is restricted to 4 %, whereas targets would have to be applied at a small distance below the wearing surface when the weak K-X-radiation would be used for excitation in combination with low Z target materials.

3.1.2. Gd-153 (97 keV- and 103 keV-γ ; 42 keV-X-X)

The short half-life of 240 d is a disadvantage. Screening of the detector crystal against direct gamma radiation is difficult.

3.1.3. Am-241 (60 keV-γ and 14 to 20 keV-X-rays). The half-life is 458 y.

α-decay leads to Np-237 yielding 60 keV-γ in approximately 40 % of all events and about as many L-X-photons in the 14-20 keV range. This combination of low energies is very useful in target excitation, since high fluorescence efficiency is obtained just above the absorption edge. Gammas of 60 keV are able to excite K-X-radiation of Z = 69 (Tm) and of lower Z. The fluorescence efficiency decreases with decreasing Z, being about 50 % in the case of Z = 40 (Zr). Fig. 2 (ref. 8) shows

that L-X radiation is becoming effective in this region, so that lower energies can also be excited with a good yield.

Two source geometries with respect to the detector may be fundamentally considered, namely a "point"-source placed on the centre of the detector, or a ring-shaped source around the detector. A central source offers the advantage of minimum intensity loss, which is compensated by the disadvantages of the decreased effective detector surface and of the higher specific source activity required. A ring-shaped source, however, can be prepared from relatively low specific activity *). In addition there is more space for screening the detector against direct radiation; a collimator can be placed in front of the detector whenever fluorescence radiation from a small area has to be detected.

For all these reasons an annular Am-241 source has been chosen, containing 1.3 mCi as Am_2O_3 electrodeposited on a Pt-ring of 2" diameter. This source has been supplied by the Radiochemical Centre, Amersham, at a price of £ 86/-. The Pt-ring has been placed on a PVC-support and covered by thin Al-foil.

3.2. Target

The choice of the target element is the chief determinant of the accuracy obtainable. In absence of any backscatter effect optimum conditions would prevail, if $\mu = 2/x$. [9]

μ ... mass attenuation coefficient of wearing layer for X-rays to be chosen $(g^{-1} \, cm^2)$

x ... surface weight of wearing layer $(g \, cm^{-2})$.

---

*) Formally, there is no difference between a ring-shaped source and a point-source of equal total activity, placed at any point on the circumference of the ring. The homogeneity of an annular source is therefore of minor importance.

Since, however, scattering of the exciting radiation cannot be avoided (cf. Chapter 5.), the characteristic X-ray energy should be as clearly separated from the backscatter peaks as possible. Furthermore X-rays should be excited with a reasonable efficiency (see Fig. 2) and target material should not be too extravagant.

A silver target largely fulfils these requirements. Energy spectra recorded from rubber flooring material with target and from target alone are shown in Fig. 3. LL and UL (lower and upper level) indicate the position of the channel selected for counting.

4. APPARATUS

4.1. Detector

A NaI(Tl) scintillation crystal 1" in diameter and 1 mm thick has been chosen as the detector. This thickness is sufficient to absorb 99 % of 22.6 keV photons and affords some discrimination against unwanted primary or scattered higher energies (e.g. 90 % detection efficiency for 60 keV).

A Be-window of 0.008" (0.2 mm; 37 mg cm^{-2}) has been employed to minimize absorption prior to detection.

Figs. 4a and 4b show absorption data in the detector and the window respectively.

4.2. Measuring probe

The annular radiation source (cf. 3.1.) with support and screening on the one hand and the scintillation crystal (cf. 4.1.) plus photomultiplier and emitter-follower on the other hand have been combined in fixed position towards each other to form the measuring probe. The crystal and the photomultiplier have been contained in a separate closed unit allowing for disassembly and exchange in the experimental stage; an integral line detector can be recommended for final use. An emitter-follower has been built into the probe and connected directly to the photomultiplier anode to render the electronic signal independent of the length of cable leading to the counting device.

The source-holder contains successive absorbers of Ag, Cu and Al in order to screen off the detector against direct radiation. Characteristic X-rays excited in one of the absorbers are attenuated in the next one as much as possible in view of the limited distance between source and detector. The source-holder can be disassembled as easily as the detector part of the measuring probe. The measuring probe weighs about 1.5 kg.

Fig. 5. contains details of the measuring probe. Rings 4, 5 and 6 have the screening function just described. The height of spacing ring 7 has been established empirically to yield a maximum signal/background ratio. Ring 2 protects the source against the hazard of damage and decreases the radiation dose from handling the probe to less than 2 mr/h. Ring 2 also determines the

size of the irradiated area. In the case of a flat object such as rubber flooring a large target can be applied, with a correspondingly large probe "orifice" to yield a large fluorescence signal.

4.3. Auxiliary apparatus

The following electronic devices are required to operate the probe and to evaluate and register a suitable signal:

4.3.1. Power-supply ($\sim$ 1000 V) for the photomultiplier.

4.3.2. Power-supply (24 V) for the emitter-follower.

4.3.3. Pulse amplifier.

4.3.4. Pulse-height analyzer.

4.3.5. Counting instrument.

4.3.6. Optional: a device to record the reading of the counting instrument on paper.

ad 4.3.4.

Two basically different ways can be considered for selecting a certain narrow X-ray energy band for counting, namely electronic single-channel discrimination and the "balanced filters" technique.

The latter procedure is based on the application of two different element filters with absorption edges just below and above the energy in question. With adjustment of the thickness of the filters so that attenuations are equal below the lower absorption edge and above the higher absorption edge, successive measurements, first with one filter and then with the other, will eliminate all but the pass-band of energies between the two absorption edges[1,2a].

Advantage: Non-electronic discrimination and thus good stability.

Disadvantage: The ratio of absorption coefficients is not constant in a broad energy band, so that electronic discrimination by means of at least a wide channel is necessary in any case[10]. Two counting procedures are necessary. Furthermore, each target would require another set of filters, which makes the method less suitable for general use, notwithstanding the relative advantage obtainable in one specially developed application.

The choice of a good electronic sliding one-channel or a multichannel analyzer offers the possibility of scanning the total energy distribution and checking the channel position, which is most useful in development and final performance of the method.

Since the whole complex of auxiliary devices should be compact and portable, a Baird-Atomic one-channel analyzer, type 530, has been chosen. Supplies for high and low tension (4.3.1., 4.3.2.), amplifier (4.3.3.), analyzer (4.3.4.), counter and timer (4.3.5.) are contained in this instrument, the dimensions of which are 44 x 38 x 15 cm^3, the weight 18 kg, and the price about £ 900/-. The possibility of scanning the pulse height distribution is present; a channel can be set to pass over the whole spectrum automatically in 100 steps of a preset time. In order to maintain recorded spectra, a small ratemeter (25 x 23 x 9 cm^3) has been built, which can be connected to the analyzer output to transmit an analogue signal to a recorder (4.3.6.).

A bloc scheme of the total measuring device as applied in the development of the method is presented in Fig. 6. The probe and the analyzer alone can be used in actual routine measurements, where counts in a predetermined channel can be read on the BA scaler.

5. THEORETICAL BACKGROUND

The signal recorded in single-channel scintillation counting has a number of constituents. These are, with remarks concerning our experiments shown in parentheses:

5.1. I_f = count rate due to target X-fluorescence radiation (silver KX-rays)

5.2. I_t = count rate due to source radiation, backscattered in target (silver)

5.3. I_{bs} = count rate due to source radiation, backscattered in object (rubber)

5.4. I_d = count rate due to radiation direct from source (americium-241)

5.5. I_b = count rate due to source radiation, scattered in backing behind target (concrete in practical experiment, air in laboratory set up).

The signal I is the sum of these constituents.

Attenuation of low energy radiation may be caused by photo-electric absorption or scattering, symbols τ and σ. The total mass attenuation coefficient is denoted by $\mu = \tau + \sigma$.

These coefficients are functions of energy E and atomic number Z, and therefore the following indices are used: σ_E^Z and μ_E^Z.

Subscript E will be replaced by e (exciting radiation energy), f (fluorescence radiation energy) and bs (backscattered radiation energy). Superscript Z will refer to t (target element) and r (object material, rubber). In the case of a composite such as rubber, the effective mass attenuation coefficient has to be used:

$$\sigma^r = \Sigma \sigma_i^r \, p_i \quad \text{and} \quad \mu^r = \Sigma \mu_i^r \, p_i \tag{1}$$

where p_i represents the weight percentage of the i-th element with mass attenuation coefficient μ_i.

The target being pure element and other fluorescence not being involved:
$$\tau_{e,K}^t = \tau_K = \text{photo-electric mass attenuation coefficient for K-shell in target}$$
material and exciting radiation.

Other symbols used are:

Ω = overall geometric efficiency factor for fluorescence and backscattered radiation in target.

Ω' = idem for backscattered radiation in object.

φ_E = fraction of quanta of energy E found within the selected energy band (channel fraction, selected by single-channel analyzer).

ε = detector efficiency (window transmission and crystal efficiency) for energy selected by single-channel analyzer.

ω_K = fluorescence yield in K-shell.

N_o = output of the source (number of quanta emitted per second in 4π steradians).

The significance of all symbols is summarized in Table I on page 16, which also contains numerical values.

5.1. X-fluorescence radiation

Incident γ-quanta may cause vacancies in the electron shells of the target material (photo-electric absorption). Mainly K-shell electrons are ejected if incident energy exceeds the K-shell binding energy.

The probability for this process to occur is expressed as a cross-section (barns/atom) or as a mass attenuation coefficient $\tau_K (cm^2/g)$. These vacancies are instantaneously ($\approx 10^{-8}$ sec) filled by electrons of L, M, etc. shells, in most cases with emission of a photon, the energy of which equals the difference in binding energies of both shells and is called the characteristic X-radiation. For silver, K-shell binding energy is 25.5 keV and the KX-quanta have an energy of 22.6 keV.

The probability that a vacancy results in a KX-photon is called ω_K, the fluorescence yield for the K-shell.

As the intensities of incident γ-rays and fluorescence KX-photons are both attenuated in the target material, the count rate contribution of fluorescence X-rays increases with target thickness to a saturation value

$$I_{f,sat} = N_o \Omega \varepsilon \varphi_f \frac{\omega_K \tau_K}{\mu_e^t + \mu_f^t} \tag{2}$$

at target saturation thickness. See Appendix I, ad 5.1.

5. THEORETICAL BACKGROUND

The signal recorded in single-channel scintillation counting has a number of constituents. These are, with remarks concerning our experiments shown in parentheses:

5.1. I_f = count rate due to target X-fluorescence radiation (silver KX-rays)

5.2. I_t = count rate due to source radiation, backscattered in target (silver)

5.3. I_{bs} = count rate due to source radiation, backscattered in object (rubber)

5.4. I_d = count rate due to radiation direct from source (americium-241)

5.5. I_b = count rate due to source radiation, scattered in backing behind target (concrete in practical experiment, air in laboratory set up).

The signal I is the sum of these constituents.

Attenuation of low energy radiation may be caused by photo-electric absorption or scattering, symbols τ and σ. The total mass attenuation coefficient is denoted by $\mu = \tau + \sigma$.

These coefficients are functions of energy E and atomic number Z, and therefore the following indices are used: σ_E^Z and μ_E^Z.

Subscript E will be replaced by e (exciting radiation energy), f (fluorescence radiation energy) and bs (backscattered radiation energy). Superscript Z will refer to t (target element) and r (object material, rubber). In the case of a composite such as rubber, the effective mass attenuation coefficient has to be used:

$$\sigma^r = \Sigma \sigma_i^r \, p_i \quad \text{and} \quad \mu^r = \Sigma \mu_i^r \, p_i \tag{1}$$

where p_i represents the weight percentage of the i-th element with mass attenuation coefficient μ_i.

The target being pure element and other fluorescence not being involved:

$\tau_{e,K}^t = \tau_K$ = photo-electric mass attenuation coefficient for K-shell in target material and exciting radiation.

Other symbols used are:

Ω = overall geometric efficiency factor for fluorescence and backscattered radiation in target.

Ω' = idem for backscattered radiation in object.

φ_E = fraction of quanta of energy E found within the selected energy band (channel fraction, selected by single-channel analyzer).

ε = detector efficiency (window transmission and crystal efficiency) for energy selected by single-channel analyzer.

ω_K = fluorescence yield in K-shell.

N_o = output of the source (number of quanta emitted per second in 4π steradians).

The significance of all symbols is summarized in Table I on page 16, which also contains numerical values.

5.1. X-fluorescence radiation

Incident γ-quanta may cause vacancies in the electron shells of the target material (photo-electric absorption). Mainly K-shell electrons are ejected if incident energy exceeds the K-shell binding energy.
The probability for this process to occur is expressed as a cross-section (barns/atom) or as a mass attenuation coefficient $\tau_K(cm^2/g)$. These vacancies are instantaneously ($\approx 10^{-8}$ sec) filled by electrons of L, M, etc. shells, in most cases with emission of a photon, the energy of which equals the difference in binding energies of both shells and is called the character- istic X-radiation. For silver, K-shell binding energy is 25.5 keV and the KX-quanta have an energy of 22.6 keV.

The probability that a vacancy results in a KX-photon is called ω_K, the fluorescence yield for the K-shell.

As the intensities of incident γ-rays and fluorescence KX-photons are both attenuated in the target material, the count rate contribution of fluo- rescence X-rays increases with target thickness to a saturation value

$$I_{f,sat} = N_o \Omega \varepsilon \varphi_f \frac{\omega_K \tau_K}{\mu_e^t + \mu_f^t} \tag{2}$$

at target saturation thickness. See Appendix I, ad 5.1.

Both exciting and fluorescence radiations pass through the wearing object of surface weight x $(g\ cm^{-2})$ with mass attenuation coefficients μ_e^r and μ_f^r respectively, so that the intensity of the fluorescence contribution finally reaching the detector can be written as

$$I_f = N_o \Omega \varepsilon \varphi_f \frac{\omega_K \tau_K}{\mu_e^t + \mu_f^t} \exp\left[-(\mu_e^r + \mu_f^r)x\right] \qquad (3)$$

5.2. Backscatter in target

Competitive with photo-electric absorption (5.1.) is the process of scattering of the exciting radiation (cross-section σ_e^t). In the scattering process energy is lost and γ-quanta are scattered into the detector with a broad energy distribution. Part of this distribution will enter the channel, namely a channel fraction φ_{bs}.

Scattered radiation also reaches saturation. By analogy with formula (2) we find

$$I_{t,sat} = N_o \Omega \varepsilon \varphi_{bs} \frac{\sigma_e^t}{\mu_e^t + \mu_{bs}^t} \qquad (4)$$

see Appendix I, ad 5.2.

For the contribution to the total measured count rate we find a formula similar to (3):

$$I_t = N_o \Omega \varepsilon \varphi_{bs} \frac{\sigma_e^t}{\mu_e^t + \mu_{bs}^t} \exp\left[-(\mu_e^r + \mu_{bs}^r)x\right] \qquad (5)$$

5.3. Backscatter in object

In addition to scatter in the target, scattering in the object under study is inevitable. A low Z material like rubber gives rise to relatively large amounts of backscattered radiation. Fig. 7. provides a representation of the correlations between scattered intensity, surface weight x and atomic number Z, as measured for 60 keV.

We find for the component I_{bs}

$$I_{bs} = N_o \Omega' \varepsilon \varphi_{bs} \frac{\sigma_e^r}{\mu_e^r + \mu_{bs}^r} \{1 - \exp[-(\mu_e^r + \mu_{bs}^r)x]\} \qquad (6)$$

see Appendix I, ad 5.3.

5.4. Direct radiation from the source

There will be a continuous background of primary source radiation reaching the detector without any object or target placed under the measuring probe, partly by penetration of the shielding, partly by scattering against the materials of the probe itself. This contribution can be written as

$$I_d = N_o \alpha \varphi_e \qquad (7)$$

where α is the fraction of initial source output N_o that reaches the detector and φ_e the fraction thereof that enters the channel. I_d can be determined directly by experiment.

5.5. Backscatter in backing

When the object and the target are placed on top of a backing (like a concrete floor in an actual test), the radiation scattered from the backing will contribute to the signal. An expression for I_b is given in Appendix I, ad 5.5. and consists of a factor analogous to eq. (6) and factors expressing the attenuation of the exciting radiation through the object and the target respectively and attenuation of the scattered radiation on the way back to the detector.

The influence of this contribution may be reduced by increasing target thickness when possible; it may be neglected when air is the backing as was done in the experiment to obtain the wide range correlation curve in Fig. 8 (cf. 6.1.).

6. EXPERIMENTS

In a study to assess wear of rubber flooring material silver was chosen as target element and 60 keV-γ-radiation of Am-241 to excite its characteristic KX-rays of 22.6 keV. Typical energy spectra are shown in Fig. 3. Curve A represents the fluorescence peak produced by a silver target without an interposed object. Scattered radiation of 60 keV-γ contributes to the energy spectrum with a broad distribution around a maximum at 50 keV, in accordance with energy loss in scattering over 180°. Curve B depicts the presence of a rubber tile between target and detector: the fluorescence peak is attenuated and the backscatter count rate has increased. The selected energy range is indicated by LL and UL (lower and upper level).

6.1. Wide range correlation between detector signal and rubber thickness

In order to investigate the depth at which a target might be applied, a wide range of rubber thicknesses has been measured. These results are shown as open circles in Fig. 8. After the target had been removed, backscatter intensities were measured separately. Experimental points are indicated by squares; the residual signal at zero thickness is caused by direct radiation. The calculated differences between circles and squares are shown by crosses.

These results can be compared with the predictions in Chapter 5. In order to do so, numerical values have been established as far as possible and listed in Table I.

Since the theoretical expressions in Chapter 5 are derived on the assumption of normal incidence, corrections for effective x-values have to be made for other angles (cf. Appendix II). Curve A, representing the sum $I_{bs} + I_d$, is found from (6) and (7), provided that x-values are corrected in accordance with Appendix II. Curve B, representing the sum $I_f + I_t$ is found from (3) and (5) in the same way.

Table I

Numerical values for evaluation of equations in Chapter 5.

symbol	significance	value	unit	method
μ_e^r	total mass att. coeff. for exciting radiation, in object	0.322	cm^2/g	calculated (1) *)
μ_e^r	total mass att. coeff. тor exciting radiation, in object	0.31	"	measured
μ_f^r	total mass att. coeff. for fluorescence radiation, in object	2.28	"	calculated (1) *)
μ_f^r	total mass att. coeff. for fluorescence radiation, in object	2.3	"	measured
μ_{bs}^r	total mass att. coeff. for backscattering radiation, in object	0.430	"	calculated (1) *)
μ_e^t	total mass att. coeff. for exciting radiation, in target	5.67	"	Table 11)
μ_f^t	total mass att. coeff. for fluorescence radiation, in target	10.8	"	Table 11)
μ_{bs}^t	total mass att. coeff. for backscattering radiation, in target	9.21	"	Table 11)
σ_e^r	scatt. mass att. coeff. for exciting radiation, in object	0.186	"	calculated (1) *)
σ_e^t	scatt. mass att. coeff. for exciting radiation, in target	0.32	"	Table 11)
τ_K	K-photoelectric mass att. coeff. for exciting radiation, in target	4.71	"	Table 12)
ω_K	K-shell fluorescence yield in target	80.6	%	Table 13)
ε	detection efficiency from 10 to 33 keV	98	%	calculated
φ_f	channel fraction of fluorescence radiation	79.5	%	measured
φ_{bs}	channel fraction of backscattering radiation	32.0	%	measured
φ_e	channel fraction of exciting radiation, direct from source	21.4	%	measured

*) cf. Appendix III.

Since quantities N_o, Ω , Ω' and α cannot be determined directly, the theoretical curves A and B were normalized to the experimental values at $x = 0$ and $x = \infty$ respectively (see Appendix IV).

Curve C, drawn as the sum of curves A and B is in good agreement with the experimental points (circles in Fig. 8). Maximum accuracy in the system under consideration can be obtained if x <200 mg cm^{-2}. Beyond 1000 mg cm^{-2} (5.5 mm since $\rho = 1.83$ g cm^{-3}) backscatter plays a major role. For the material under study, flooring tiles 1.6 mm thick ($\sim$ 300 mg cm^{-2}), accuracy is still satisfactory.

6.2. Small range calibration of detector signal versus rubber thickness

The investigation has been directed towards detection of very small changes of a thickness around 1.5 mm. A calibration curve has therefore been measured in more detail in the region of interest (240 - 300 mg cm^{-2} = 1300 - 1600 μm). For this purpose the thicknesses of a number of rubber disks were slightly reduced by abrasion to a different degree and determined by weighing. A suitable series of samples has been selected to serve as objects for a calibration curve (Fig. 9). The sensitivity of the method can be read from this line in absolute or relative terms.

The absolute sensitivity, equal to the slope of the curve in the region of interest, is 2.02 cps/μm with a standard deviation of 0.04 cps/μm. In a counting time of 2×100 sec, 1.3×10^6 counts are collected, with a 3σ-error of 18 cps. This yields an absolute accuracy of 9 μm in 200 sec.

The relative sensitivity S and relative accuracy R can, for instance, be calculated according to Clayton and Cameron[2a]

$$S = \frac{\Delta I/I}{\Delta x/x} ; \qquad R = 200/S\sqrt{N}\%.$$

In our case $S = \dfrac{400 \text{ cps}/6400 \text{ cps}}{200\ \mu m/1600\ \mu m} = 0.5$ (cf. Fig. 9)

and consequently $R = 200/0.5 \sqrt{2 \times 6.4 \times 10^5} = 0.35 \%.$

6.3. Accelerated wear experiment

In order to check the performance of the apparatus and the principle of the method in an actual experiment, accelerated wear was simulated on a lathe. A silver target was fixed on a leveled aluminium support and covered with a sample of the rubber flooring under study. The sample was left in this position during the experiment. A cutter was set to grind off the sample 25 μm at a time.

After each operation the count rate was measured with the probe after displacement of the support into a measuring position. A mechanical gauge, accurate to within $\pm$ 5 μm, was used to measure the distance between the support and the surface of the sample, so that the thickness decrease effectuated could be measured independently. This enabled us to plot the count rate against the wear (Fig. 10). The indicated uncertainties are the counting statistics ($\pm$ 3σ) and the accuracy of reading the gauge ($\pm$ 5 μm).

The next step was to find the wear from the count rates by means of the calibration curve (Fig. 9). This is the procedure to be followed normally, when independent measurement is not possible.

A check can be made (Fig. 11) by plotting the wear, measured by the mechanical gauge, against the wear assessed by the γ-X-fluorescence method. A straight curve with slope 45° seems to be a good fit.

6.4. Test under practice conditions

In addition to and partly simultaneously with the laboratory experiments a test under practice conditions was conducted in order to demonstrate that the method can be applied to flooring material which may be left in position during the test.

6.4.1. Preparations

Rubber tiles (25 x 25 x 0.16 cm^{3}) were chosen and silver targets were glued onto the back-sides. These targets were 200 μm thick according to saturation thickness for fluorescence as well as for backscatter (see Appendix I ad 5.1. and ad 5.2.). The other dimensions were 10 x 10 cm^{2} to meet amply the measuring aperture of the probe (cf. Fig. 5).

A first measurement was made in the laboratory and was compared with the calibration curve to yield a value for the thickness at the

place of the target.

It is desirable to carry out wear experiments at places of very high traffic density. W.J. Warlow et al.[14], for instance, have been able to choose the flooring below three ticket office windows in a London underground station for a comparative study of flooring materials. In our case the testing of the method, not the wear of the flooring, was of interest. So a relatively favourable place was found in the office building of the rubber factory that supplied the tiles. A turning point in a flight of steps offered a level area where the nine measuring places were laid out in a pattern as shown in Fig. 12.

In seven cases the targets were placed in the middle of a tile, in one case close to an edge; a ninth target was placed under four adjacent corners of four tiles, yielding a total of nine measuring places.

Site 1 was chosen in a corner at a window where no traffic was expected, to serve more or less as a standard. Sites 2 through 5 were laid down on the top of the staircase , providing a chance to recognize a traffic pattern. Sites 6 through 9 were positioned at places where maximum traffic could be expected. Site 8 was to act as a check on the performance of site 9.

An arrangement was made with the maintenance supervisor that no wax would be applied and just water and soap would be used for cleaning the floor.

6.4.2. Measurements

Thirteen measurements were taken during a period of nearly one year. In the beginning intervals of about two weeks were chosen. Later intervals of one to two months were considered sufficient in view of the small amount of wear.

The procedure followed each time was rather simple. After arrival at the office building the apparatus needed a warming-up period of about one hour before the amplification of the analyzer was stabilized; this could be judged by measuring the count rate in the selected channel, using a standard consisting of a piece of rubber flooring material with a silver target attached to it. This

provided a way to account for small aberrations of the channel po-
sition or of the amplification factor in the course of the measure-
ments. The energy selection of the channel is indicated in Fig. 3.

Measurements of 3 x 100 sec were then made at each site, by
simply placing the measuring probe on the floor in the position shown
in Fig. 5. The signal thus obtained yielded an average over some
18 cm^2 of flooring material.

6.4.3. Results

The results of all measurements taken at the nine sites have
been summarized in Fig. 13 as rectangles, the longer sides of which
indicate 5 times the standard deviations. In the last curve (A) the
average wear behaviour of sites 2 through 8 has been plotted. Of
course the points spread more than should be expected from counting
statistics, because the readings are affected by stains and dirt,
and therefore by the thoroughness of cleaning, as well as by the
inhomogeneity of the traffic density.

The series of measurements at 161 days yielded values which were
not expected. At nearly all sites a decrease in signal was measured,
corresponding to an average increase in thickness of some 50 μm in-
stead of the expected decrease of 10 μm. Four weeks later, at 189
days, an average wear was found in agreement with the wear rate es-
tablished, but still on a level of an extra 60 μm thickness, as indi-
cated by the solid line between 150 and 220 days in Fig. 13 (A).
Control site 1, however, displayed a sharp rise in signal at both 161
and 189 days. After inquiry the first aberration could be traced back
to an application of wax in spite of given orders. A change in
maintenance firm was responsible for this misunderstanding. After
thorough cleaning of the flooring with a detergent prior to the next
measurement, values were back to normal again.

At the same time control site 1 reassumed its normal value; the
deviations at this site remain unexplained. Therefore the two
measurements at 161 and 189 days have been left out of consideration,
as indicated in Fig. 13 by dotted lines.

By a least squares fit, omitting the open rectangles at 161
and at 189 days, straight lines have been drawn to indicate the
average wear rate at each site. In Fig. 12 the wear rates (in arbi-.
trary units, de facto in μm per year) have been plotted on the
places where they have actually been measured. A traffic pattern
can clearly be recognized, while the measuring site 9, under the
adjacent corners of four tiles, seems unsuitable, as is demonstrated
by site 8.

Fig. 14 shows the average wear rates normalized to wear zero
at zero time. From the points on these lines at 336 days the wear
assessed by the γ-X-fluorescence method can be read (see Table II).
The standard deviations have been calculated from the distribution
of the measured thicknesses. They vary from 21 μm (16.7 %) in the
case of site 3, where points scatter most, to 11 μm (7.4 %) in the
case of site 6 where little scattering is observed.

When the experiment was stopped after 336 days, an attempt was
made to recover the tiles in order to state the wear independently
by a mechanical measurement. In this attempt sites 1, 5 and 9 were
destroyed. The other tiles have been cut along the silver targets.
Then the targets have been removed from the tiles by dissolving the
glue. After a drying period the thickness of the tiles could be
measured mechanically at the same spots where the γ-X-fluorescence
measurements have been taken. The solvent was known to reduce the
weight of the rubber composition by 1.8 % so the thickness measured
has been corrected for this effect. Results and standard deviations
are shown in Table II.

The differences between wear assessed by the γ-X-fluorescence
method and the mechanical measurements are listed in Table II also.

The standard deviation in the difference has been calculated
according to S.D. $= \sqrt{S.D._1^2 + S.D._2^2}$.

Table II[*]. Results and standard deviations S.D. of the test under conditions of practice. All values in µm.

site nr.	γ-X-fluorescence method		mechanical method		comparison	
	wear	S.D.	wear	S.D.	difference	S.D.
1	10	11	destroyed	–	–	–
2	88	16	124	6	+36	17
3	126	21	141	4	+15	21
4	144	14	156	6	+12	15
5	124	17	destroyed	–	–	–
6	148	11	174	16	+26	20
7	146	14	112	7	-34	16
8	120	19	130	10	+10	22
9	92	17	destroyed	–	–	–
A[**]	128	10	139	4	+11	11

Student's test, applied to the column of differences, shows that the values do not differ significantly from zero.

---

[*] Statistical calculations have been revised by Drs. M. Wigbout from Afdeling Bewerking Waarnemingsuitkomsten-TNO

[**] A = average of sites 2 through 8

7. DISCUSSION

The γ-X-fluorescence method of measuring wear is non-destructive and re-
quires no sampling. No radioactive products have to be left at the measuring
sites, as was done in previous studies[15]. Therefore, the method would be very
appropriate in absolute or comparative studies on resistance to wear under
practice conditions, especially when applied to measuring sites of high traffic
density.

In his study on the resistance to wear of different flooring materials,
W.J. Warlow[14] finds an average wear of 370 μm for 5 mm thick rubber flooring,
after passage of 500.000 persons with an average of 31.700 weekly. The pieces
of flooring were removed after four to six weeks, measured, and repeatedly
placed back at the test site.

With the γ-X-fluorescence method the objects could have been left in po-
sition, while the sensitivity is high enough to give a measurable effect after
a wear of 10 μm, which means after passage of 13.000 persons. Therefore twice
a week a significant difference could have been measured. Furthermore, accuracy
can be increased by using longer measuring times.

In the practical test performed in the course of our investigation, the
number of passings is not known at all. At very rough estimate perhaps some 400
people will have passed the test area per day, that is 134.400 during the period
in which the measurements were taken (336 days). The average wear assessed is
128 μm, leading to 480 μm wear for 500.000 people crossing.

This value is of the same order of magnitude as Warlow's. The higher wear
rate found in our experiments is in accordance with the choice of a medium quali-
ty of flooring material, which had been purposely selected to yield greater wear
effects.

8. CONCLUSIONS

Wear measurements on rubber can be carried out by means of γ-X-fluorescence with good accuracy, simple equipment and little preparation. The method has the advantage of being "clean" in radiological sense as well as being non-destructive, while measurements can be made successively without removing the wearing object.

The following results have been obtained:

1. (cf. 6.1., Fig. 8, Appendices II, III, IV) The correlation between the signal and the object thickness could be predicted to a sufficient degree of precision by means of an approach based upon theoretical considerations combined with experimental data at the extreme object thicknesses $x = o$ and $x = \infty$.

2. (cf. 6.2., Fig. 9) A calibration curve was established, which could be approximated by a straight line in the region of interest (1.4 - 1.6 mm rubber thickness). The slope of the curve is 2.02 ± 0.04 cps/ μm. With a measuring time of 200 sec a thickness can be read from this curve with an absolute standard deviation $\sigma = 3$ μm.

3. (cf. 6.3. Fig. 10, Fig. 11) The method was tested in an accelerated laboratory experiment on a 1.6 mm thick rubber flooring compound, simulating the wear by abrasion, while the amount of wear could be measured independently. Good agreement was obtained between γ-X-fluorescence and mechanical measurements.

4. (cf. 6.4.3, Fig. 12, Fig. 13, Table II) A test under conditions of practice was run for nearly one year with the same rubber compound in nine different measuring sites. Wear was assessed, ranging from (10 ± 11) μm for a control site with a minimum of traffic expected, to (148 ± 11) μm for a maximum. Standard deviations in the results of this practical test range from 11 to 21 μm. The main contributions to this uncertainty arise from cleaning and maintenance problems. Mechanical measurements after the termination of the practical test were in good agreement with the thickness assessed by γ-X-fluorescence.

REFERENCES

1) Kirkpatrick, P., Rev. Sci. Inst. 10, p. 186 (1939).

2) Proceedings IAEA-symposium on radioisotope instruments in industry and geophysics. SM-68/4-13, p. 73-242.

2a) Clayton, C.G. and Cameron, J.F., idem, p.15-61.

3) Karttunen, J.O. et al., Anal. Chem. 36, no. 7, p. 1277 (1964).

4) Hope, J.A. et al., Int. Journ. App. Rad. Isot. 16, p. 9 (1965).

5) Baldwin "Atomat".

6) Fischer "Betascope".

7) Hilger and Watts Ltd. "PIF-analyzer" (Portable radioIsotope X-ray Fluorescence Analyzer).

8) Cameron, J.F. and Rhodes, J.R., Nucleonics 19, no. 6, p. 55 (1961).

9) Platzek, P. and Meijer A.C., Eur. 2221 (1965).

10) Rhodes, J.R. et al., AERE-report R-3925 (1962).

11) Storm, E. et al., Gamma-ray absorption coefficients LA-2237 (1958).

12) Grodstein, G.W., NBS circular 583 (1957).

13) Wapstra, A.H. et al., Nuclear Spectroscopy Tables(1959).

14) Warlow, W.J. et al., Wear 10, p. 89 (1967).

15) Sunderman, D.N. et al., Int. Journ. App. Rad. Isot. 15, p. 269 (1964).

APPENDIX I   Comments on the formulae in Chapter 5

Ad 5.1.   A layer of thickness $\Delta\xi$ at a depth ξ in the target material con-
tributes to I_f with:

$$\Delta I_f = N_o \Omega \epsilon \phi_f \; \omega_K \tau_K \; \exp \left[-(\mu_e^t + \mu_f^t)\xi\;\right]$$

(All symbols used are defined in Chapter 5)

For the total contribution up to this depth ξ we find by integration:

$$I_f = \int_o^\xi \Delta I_f \; d\xi = \frac{N_o \Omega \epsilon \phi_f \omega_K \tau_K}{\mu_e^t + \mu_f^t} \{1 - \exp \left[-(\mu_e^t + \mu_f^t)\xi\right]\} \qquad (A1)$$

With increasing thickness, I_f asymptotically approaches to

$$I_{f,sat} = \frac{N_o \Omega \epsilon \phi_f \omega_K \tau_K}{\mu_e^t + \mu_f^t} \; ; \; \text{this is eq. (2) on page 12.}$$

This saturation count rate is reached for a thickness x, de-
termined by $(\mu_e^t + \mu_f^t) \; x > 3$.
Saturation thickness for fluorescence is therefore $x_{f,sat} > \dfrac{3}{\mu_e^t + \mu_f^t}$.

With values from Table I we find for silver:
$x_{f,sat} > 0.182 \; g \; cm^{-2} \; (>173 \; \mu m)$.

Ad 5.2.   Similar reasoning is applicable to backscatter count rates.
Substitution on the right-hand side of eq. (2) of index bs for f and
σ_e^t for $\omega_K \tau_K$ leads to eq. (4) on page 13.
For silver this backscatter saturation thickness is, with values
taken from Table I,

$$x_{t,sat} > \frac{3}{\mu_e^t + \mu_{bs}^t} = 0.220 \; g \; cm^{-2} \; (> 192 \; \mu m)$$

(cf. Fig. 7).

Ad 5.3.   For scatter in object the integral in eq. (A1) has to be taken to upper limit x (thickness of object), subscript f replaced by bs, superscript t by r, $\omega_K \tau_K$ by σ_e^r and Ω by Ω'. This leads to eq. (6) on page 14.

Ad 5.5.   For scatter in backing the integral in eq. (A1) has to be taken to upper limit x_b (thickness of backing), subscript f replaced by bs, superscript t by b and $\omega_K \tau_K$ by σ_e^b. This leads to a count rate $I_{b,o}$ for the backscatter intensity in absence of object and target:

$$I_{b,o} = N_o \Omega \varepsilon \varphi_{bs} \frac{\sigma_e^b}{\mu_e^b + \mu_{bs}^b} \{1 - \exp[-(\mu_e^b + \mu_{bs}^b)x_b]\} \qquad (A2)$$

Here σ^b and μ^b are the mass attenuation coefficients in the backing material.

When the target is placed inside the object instead of behind the object $\sigma^b = \sigma^r$ and $\mu^b = \mu^r$.

The backing being thich enough to have saturation thickness for backscatter $\left(x_{b,sat} > \dfrac{3}{\mu_e^b + \mu_{bs}^b}\right)$, the last factor in eq. (A2) is eliminated.

The intensity $I_{b,o}$ in eq. (A2) is attenuated twice: from source to backing through the object (thickness x, att. coeff. μ_e^r) and target (thickness x_t, att. coeff. μ_e^t) and back through the target (att. coeff. μ_{bs}^t) and the object (att. coeff. μ_{bs}^r) to the detector.
For the count rate due to backscatter in the backing we find therefore:

$$I_b = I_{b,o} \exp[-(\mu_e^r + \mu_{bs}^r) x - (\mu_e^t + \mu_{bs}^t) x_t]. \qquad (A3)$$

APPENDIX II   Correction on path lengths in object

The quantity x which appears in the exponential absorption factors in Chapter 5 and Appendix I represents the actual path length of the radiations through the object. These path lengths depend on the position of the source and the detector with respect to each other and to the object. They should be read as $x' = x/\sin \alpha$ and $x'' = x/\sin \beta$. Angles α and β involved are shown in Fig. 15, a schematic presentation of the situation.

β is taken constant, depending only on the aperture of the probe; α is a function of x and therefore sin α has been approximated as follows:

$$\sin \alpha = \frac{x+c}{\sqrt{(x+c)^2 + b^2}}$$

where 2b is the diameter of the annular source (b = 22 mm) and c is the minimum distance between the object and the source. (c = 10 mm) (cf. Fig. 15)

For the calculation of curves A and B in Fig. 8 the exponents in (3), (5) and (6), generally of the form $(\mu_1 + \mu_2)x$, have been substituted by

$$\mu_1 \ x/\sin \alpha + \mu_2 \ x/\sin \beta = [\ \mu_1 \cdot \frac{\sqrt{(x+c)^2 + b^2}}{x+c} + \mu_2^*] \ x$$

where $\mu_2^* = \mu_2/\sin \beta$.

APPENDIX III   Composition of the rubber compound

The composition of the rubber compound used for the flooring material under study was known by courtesy of Mr. H. de Nobel from the laboratory of the rubber. factory involved. See Table III.

Table III. Weight percentages of elements in rubber compound

Z	element	weight %	μ_e *)	μ_{bs} *)	σ_e *)
1	H	3.06	0.326	0.335	0.326
6	C	21.60	0.169	0.178	0.169
7	N	0.04	0.180	0.194	0.171
8	O	39.60	0.189	0.208	0.174
12	Mg	3.86	0.253	0.322	0.183
13	Al	7.85	0.270	0.360	0.181
14	Si	15.24	0.315	0.429	0.191
16	S	1.29	0.400	0.567	0.201
20	Ca	4.17	0.648	0.998	0.215
22	Ti	0.43	0.76	1.20	0.204
26	Fe	0.25	1.20	1.93	0.223
30	Zn	2.04	1.75	2.83	0.240
56	Ba	0.57	8.38	13.4	0.360
	rubber	100	0.3224	0.4303	0.1858

*) Values for μ_e, μ_{bs} and σ_e have been taken from ref. [11].

μ_e^r, μ_{bs}^r and σ_e^r can be computed from these values by means of formula (1).

μ_f^r (for 22.6 keV) has been found by interpolation from values calculated according to (1) for 15, 20, 30, 40, 50 and 60 keV. The result is $\mu_f^r = 2.28$ cm^2 g^{-1}; these values for μ_e^r, μ_{bs}^r, σ_e^r and μ_f^r have been listed in Table I, Chapter 6.

APPENDIX IV Normalization of curves A and B in Fig. 8

"x = o" means that only a silver target is placed under the probe; hence, target fluorescence, target backscatter and direct radiation from the source are measured: $I_{f,o} + I_{t,o} + I_d = I_1$.

Rubber saturation thickness x_{sat} is obtained when x is so large that an additional increase in x no longer increases the detector signal. In that case the measured value is $I_{bs,sat} + I_d = I_2$. With neither object nor target under the probe, I_d can be measured separately. (Care should be taken to ensure that no scattering objects other than air surround the probe.)

Subtraction of the experimental value of I_d from I_1 and I_2 yields $I_{f,o} + I_{t,o}$ and $I_{bs,sat}$ respectively. The ratio $I_{f,o}/I_{t,o}$ (for x = o) can be found by means of (3) and (5) so that the two count rates $I_{f,o}$ and $I_{t,o}$ can also be known separately.

The four count rates $I_{f,o}$, $I_{t,o}$, $I_{bs,sat}$ and I_d were used to calculate the contributions I_f, I_t and I_{bs} for other values of x, making allowance for the correction mentioned in Appendix II. Finally they were taken two by two for comparison with measured values for other values of x. (See Fig. 8.)

It can be stated that measuring I_1, I_2 and I_d suffices to predict the correlation between the signal and the object thickness to a high degree of precision.
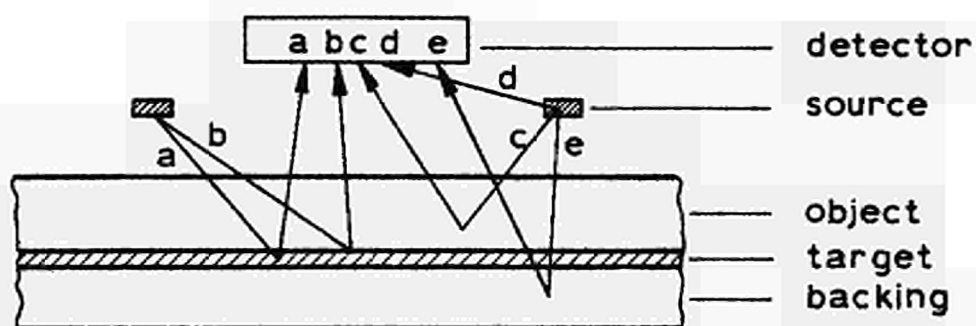
a : characteristic target X rays

b : radiation scattered in target

c : radiation scattered in object

d : direct radiation through shielding and scattered
by materials of probe

e : radiation scattered in backing

Fig. 1 SCHEMATIC INDICATION OF THE METHOD WITH
DIFFERENT CONTRIBUTIONS TO DETECTOR SIGNAL.
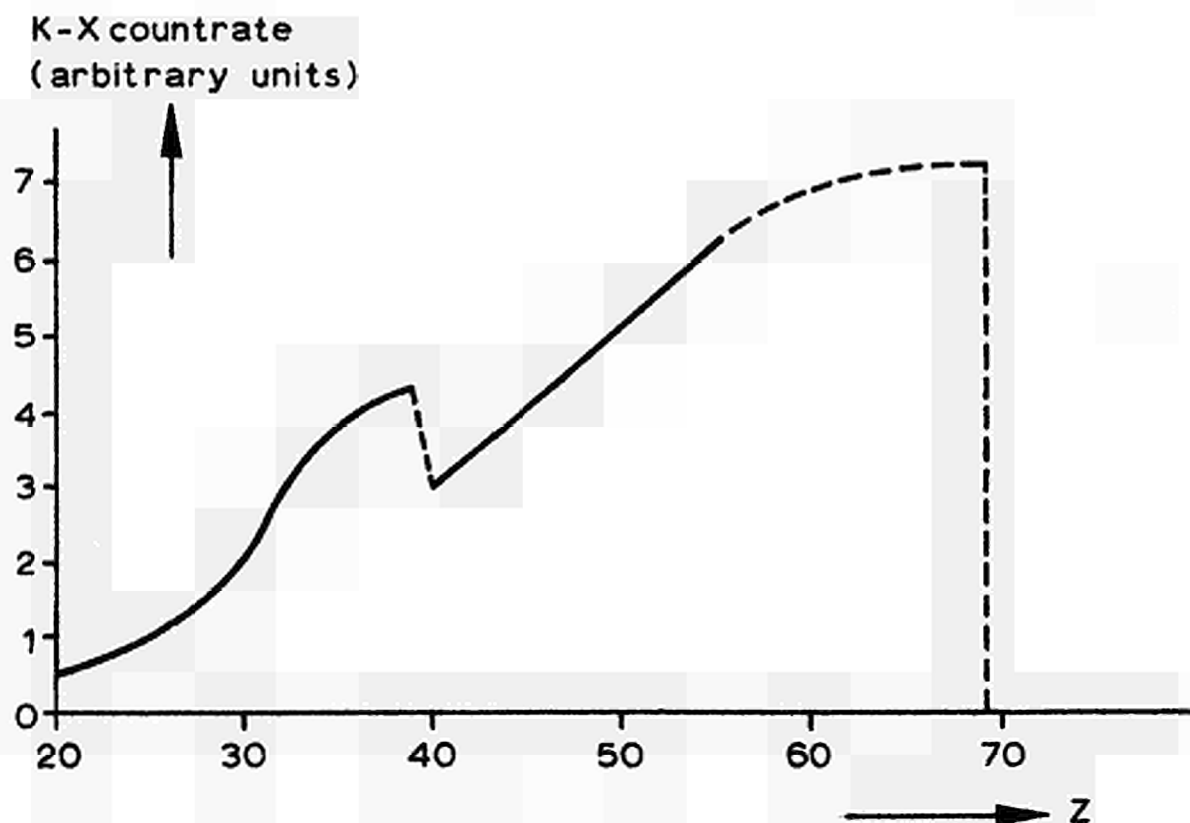
Fig. 2 RELATIVE FLUORESCENCE EFFICIENCY FOR ^{241}Am
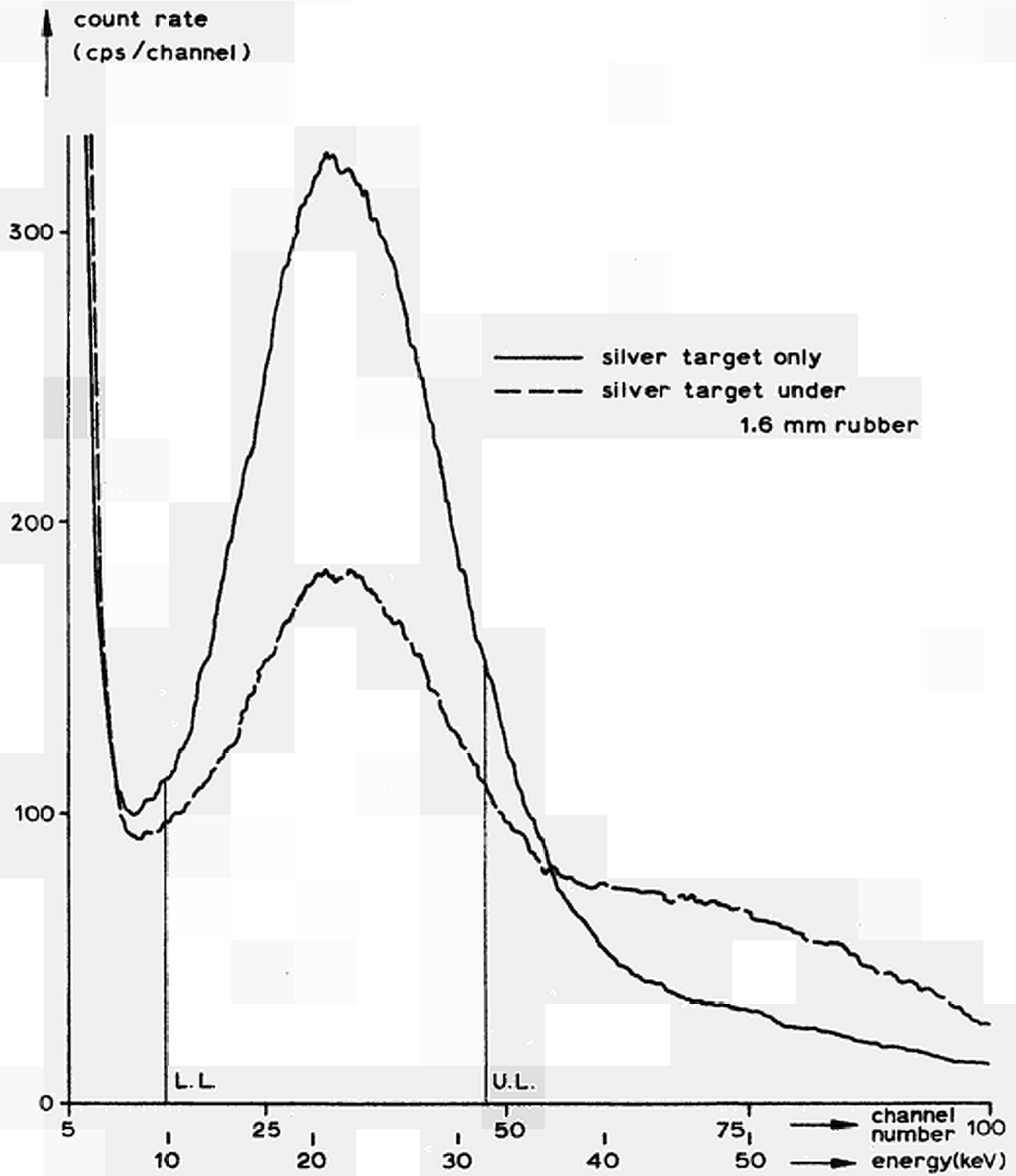
Fig. 3 ENERGY SPECTRA OF SILVER-TARGET WITH AND WITHOUT WEARING OBJECT.
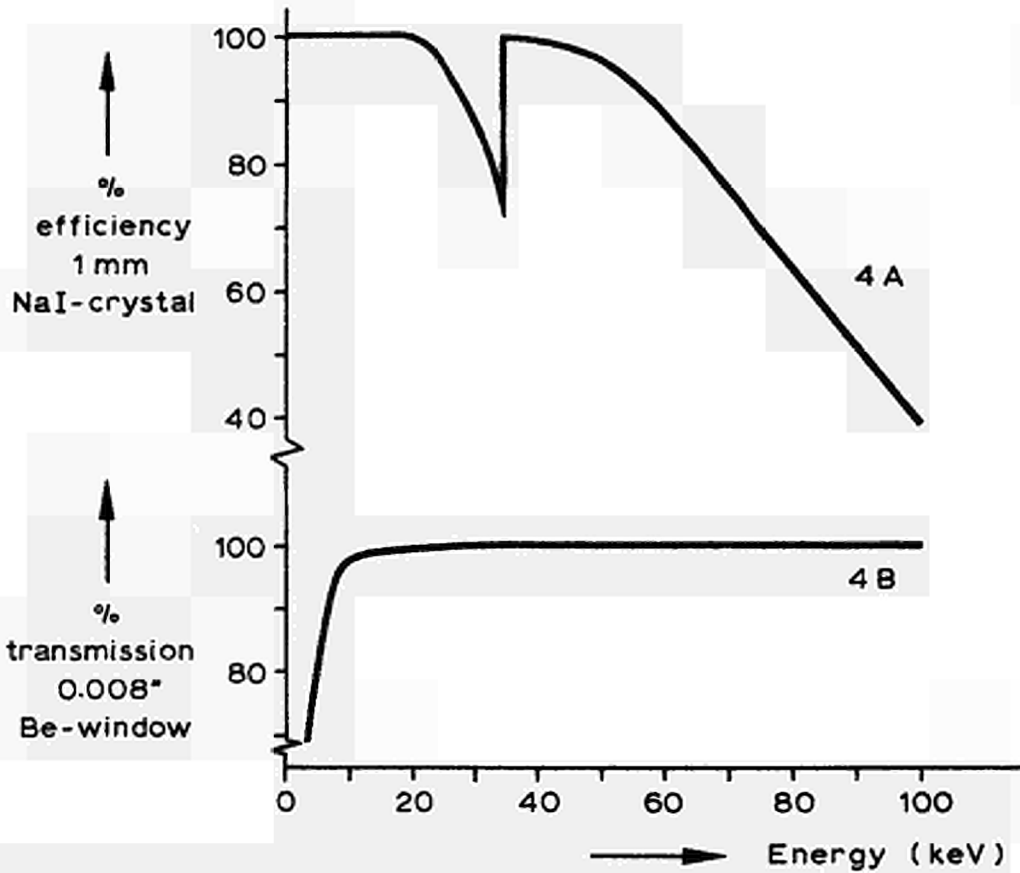
Fig. 4 ABSORPTION DATA ON CRYSTAL AND WINDOW.
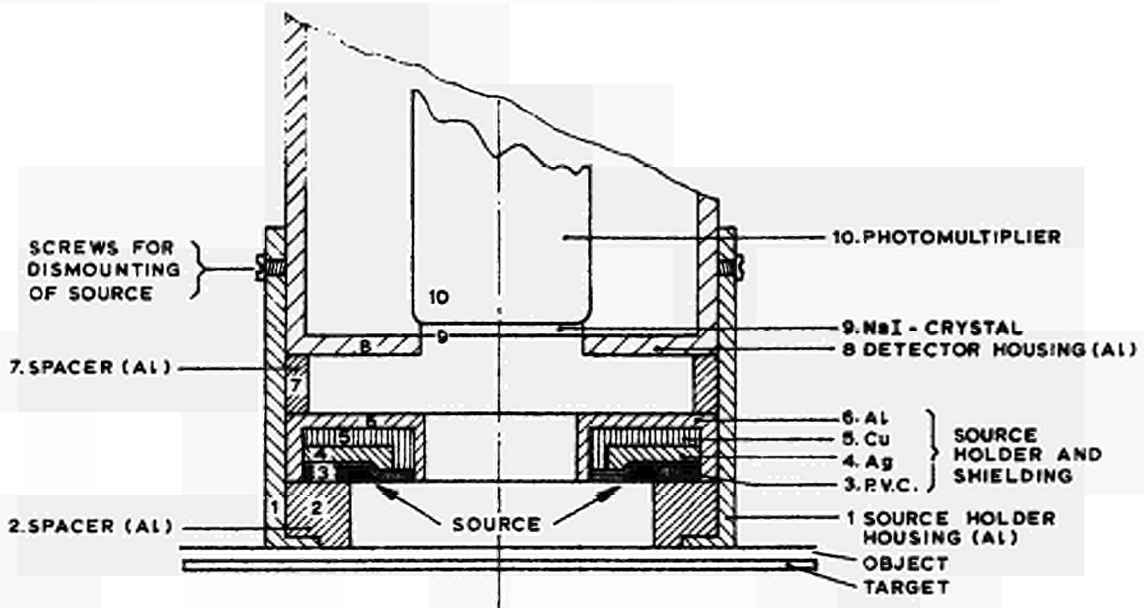
Fig. 5 GEOMETRICAL ARRANGEMENT OF PROBE (SCALE 1:1)
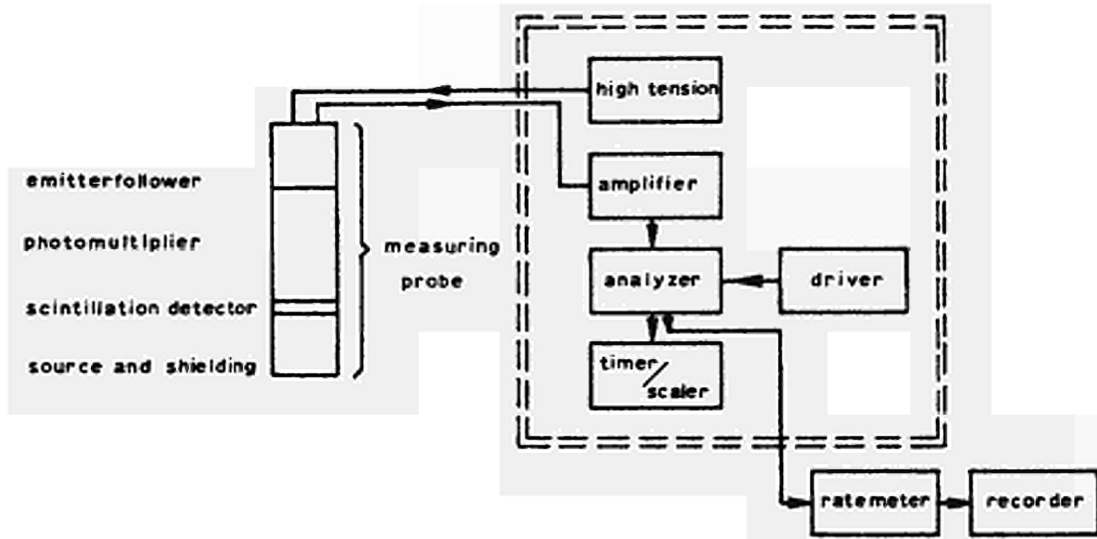
Fig. 6   BLOCKSCHEME OF APPARATUS.
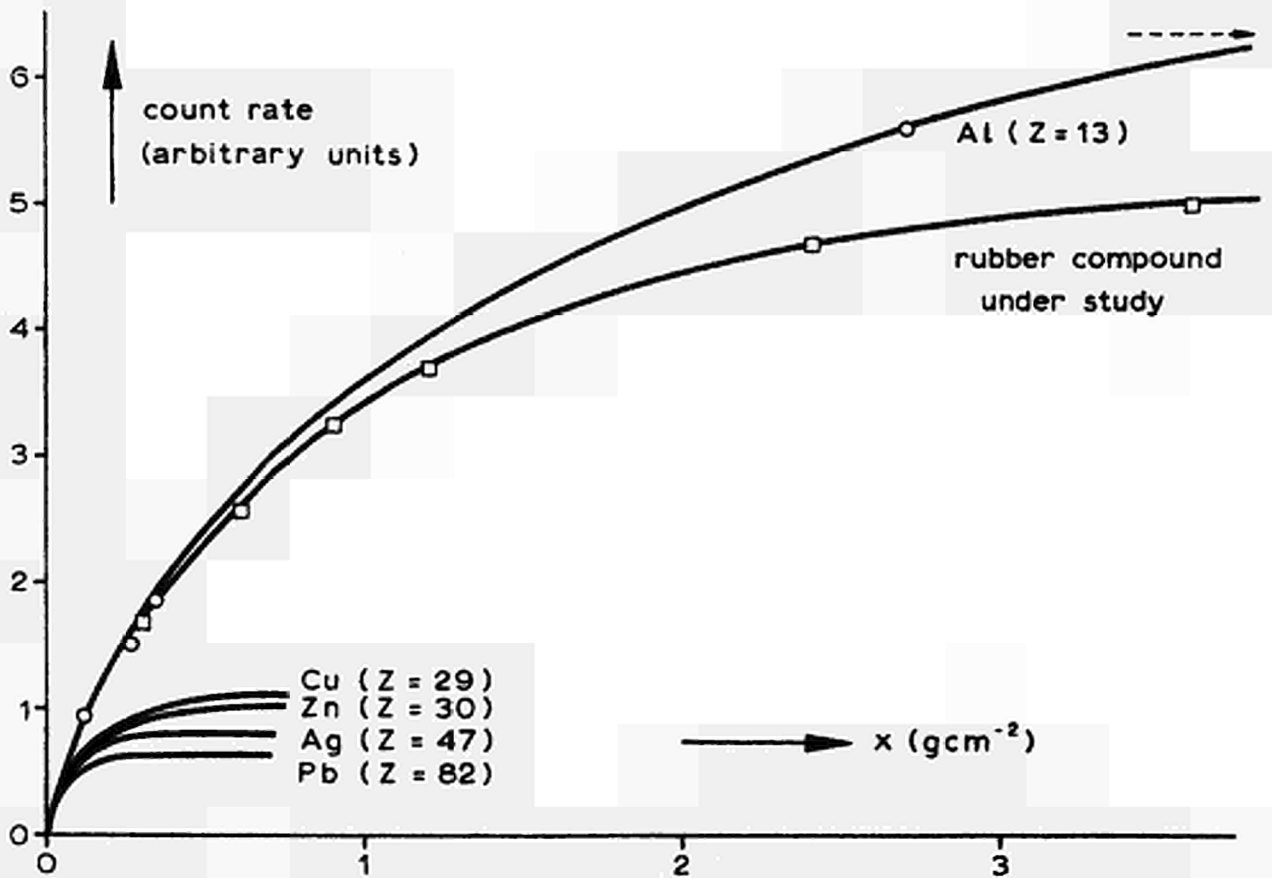
Fig. 7   RELATIVE BACKSCATTER INTENSITY FROM 60 keV-γ's AS A FUNCTION OF x AND Z
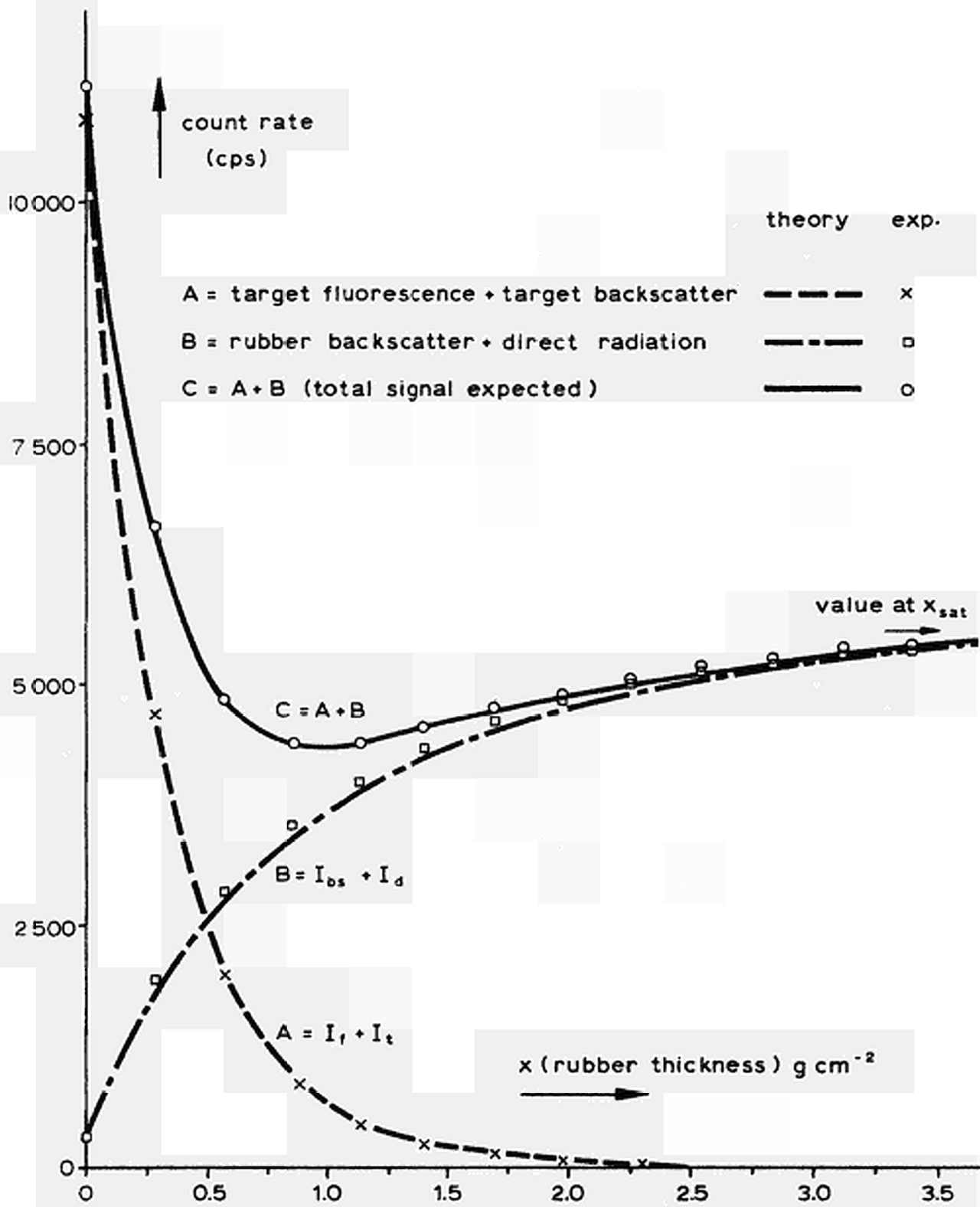
Fig. 8 CORRELATION BETWEEN COUNT RATE AND RUBBER THICKNESS

count rate
(cps)

time: 200 sec.

7 000

6 800

6 600

6 400

1350   1400   1450   1500   1550   1600   1650

x (rubber thickness) μm
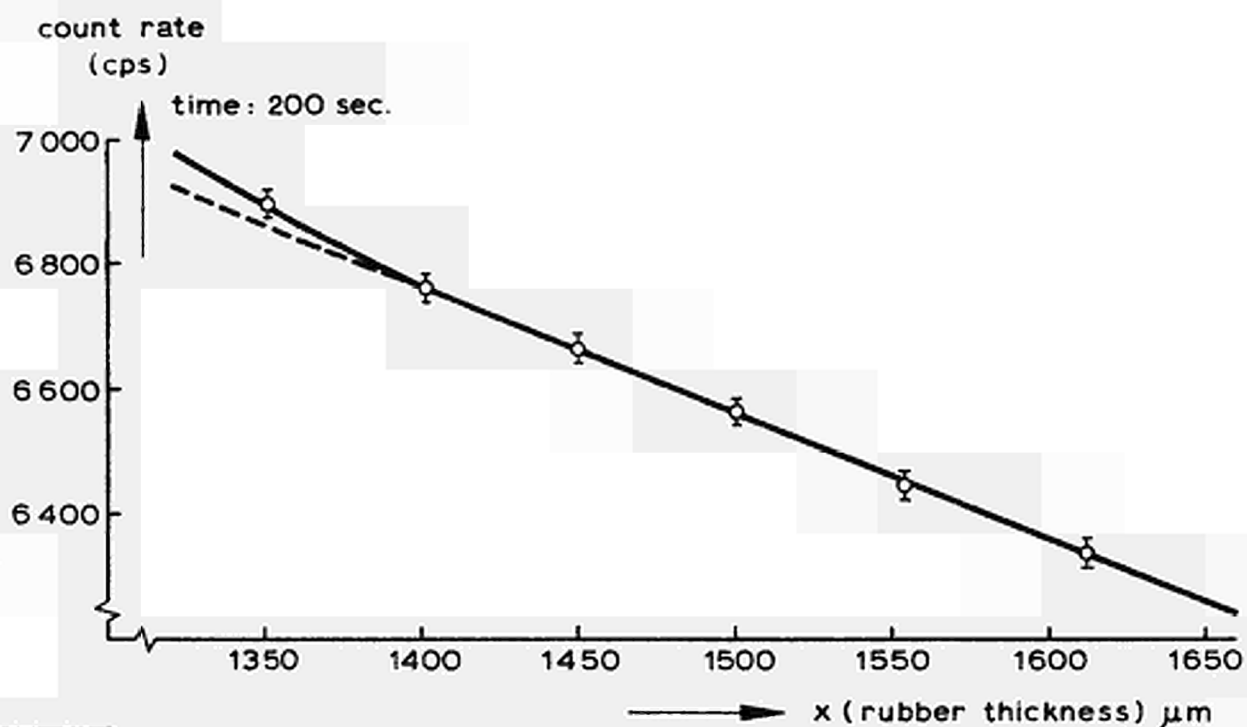
Fig. 9   CALIBRATION   CURVE   IN   REGION   OF   INTEREST

count rate
(cps)

time: 200 sec.

6900

6800

6700

6600

6500

6400

0   50   100   150   200   250

Δx (wear in μm, measured with gauge)
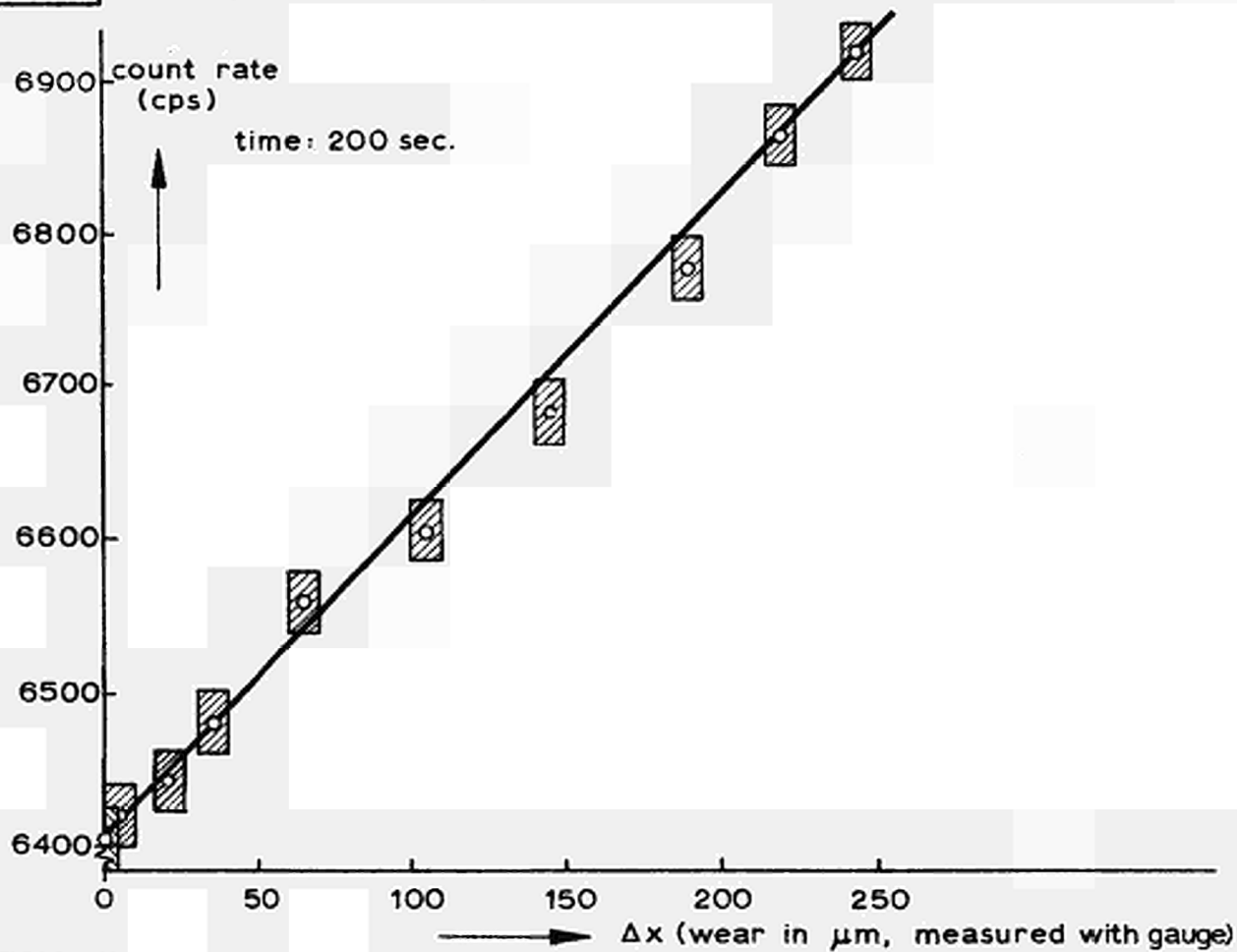
Fig. 10   ACCELERATED   WEAR   EXPERIMENT.
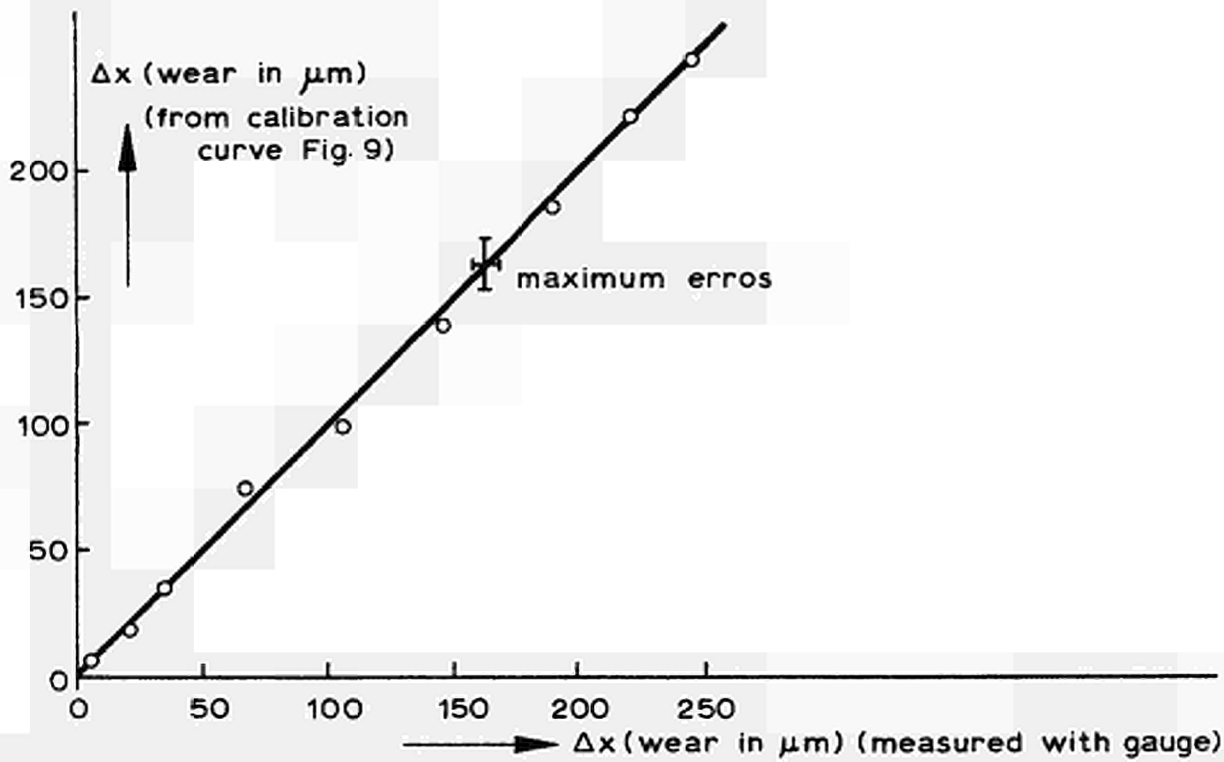
Fig. 11 CONTROL OF WEAR ASSESSED BY γ-X-FLUORESCENCE METHOD
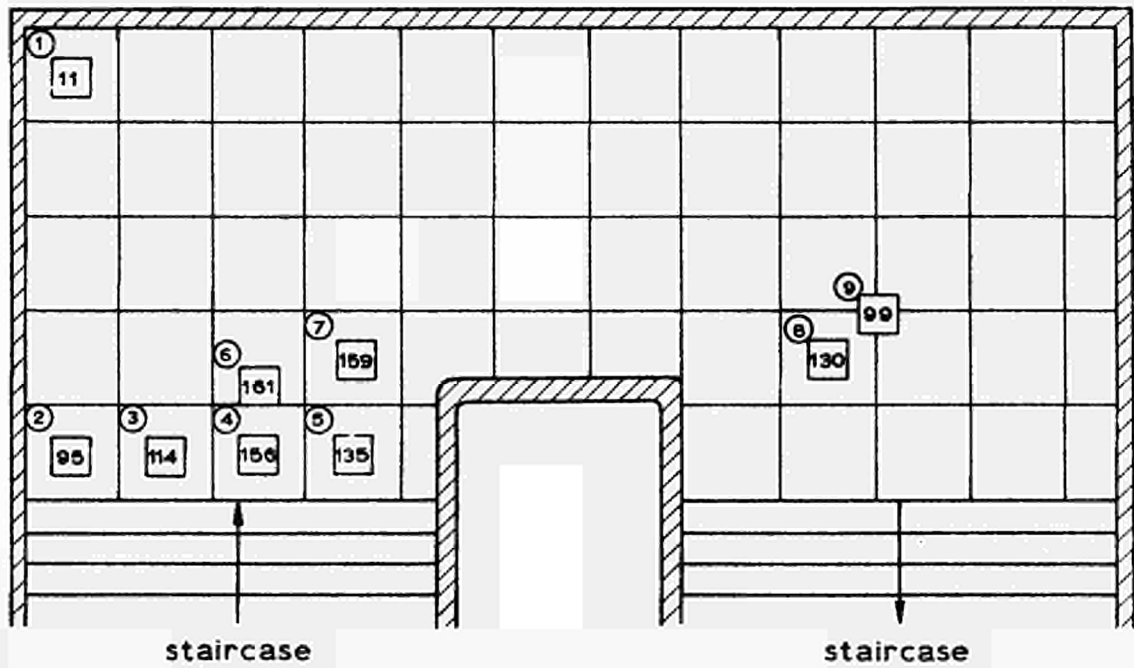
Fig. 12 POSITIONS OF MEASURING SITES, WITH INDICATION OF WEAR IN μm PER YEAR.(SCALE 6:100)
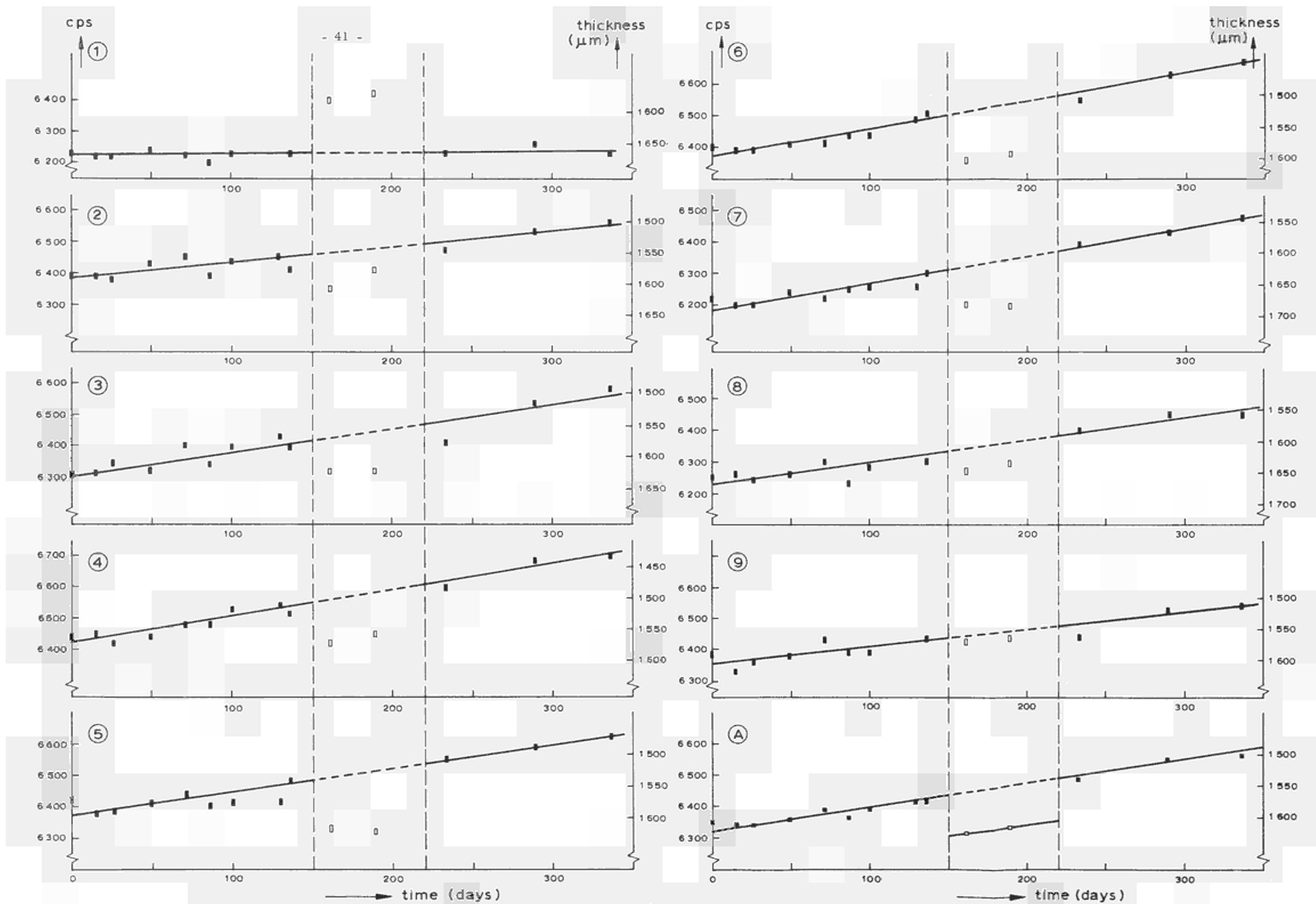
Fig. 13   SURVEY OF MEASUREMENTS AT NINE TESTSITES. Ⓐ IS AVERAGE OF SITES ②-⑧
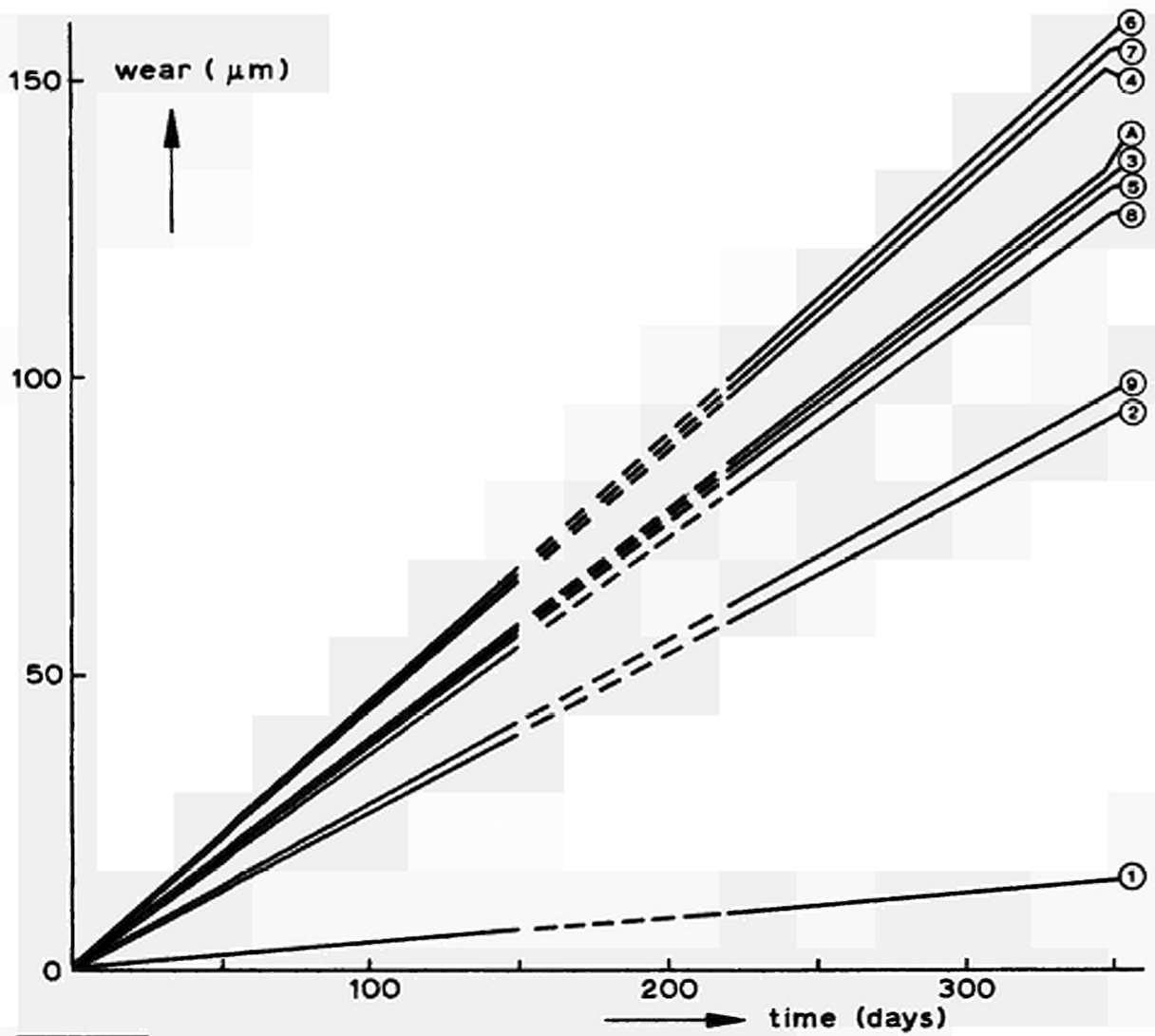
Fig. 14   WEAR RATES TAKEN FROM FIG. 13
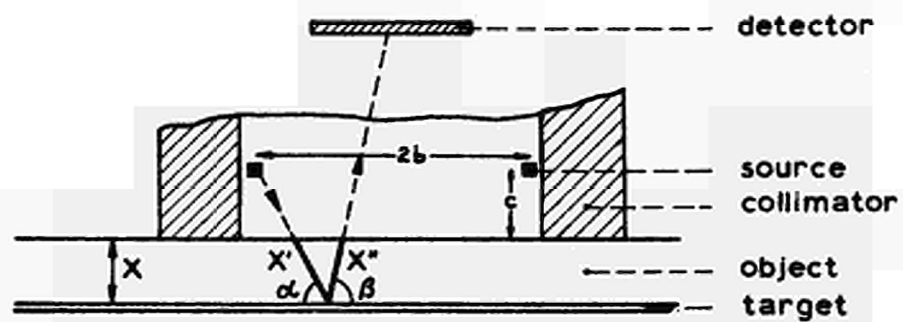
Fig. 15   SCHEMATIC PRESENTATION OF PATH LENGTHS IN OBJECT
(see Appendix II)
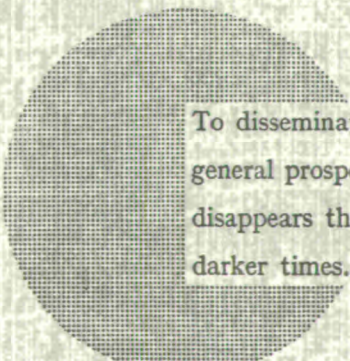
To disseminate knowledge is to disseminate prosperity — I mean general prosperity and not individual riches — and with prosperity disappears the greater part of the evil which is our heritage from darker times.

Alfred Nobel

SALES OFFICES